Dissociative adsorption of H_2 on Cu(100): Fixed-site calculations for impact at hollow and top sites

R. C. Mowrey[a)]
Theoretical Chemistry Section, Code 6179, Naval Research Laboratory, Washington, DC 20375-5342

G. J. Kroes
LIC, Gorlaeus Laboratoria, Rijksuniversiteit Leiden, Postbus 9502, 2300 RA Leiden, The Netherlands

E. J. Baerends
Theoretische Chemie, Vrije Universiteit, De Boelelaan 1083, 1081 HV Amsterdam, The Netherlands

(Received 1 December 1997; accepted 20 January 1998)

The reaction of H_2 on Cu(100) is studied using a wave-packet method to solve a four-dimensional quantum mechanical model for impact on the high-symmetry hollow and top sites. The potential energy surface (PES) is a fit to the results of density functional calculations treating a periodic overlayer of H_2 on a Cu slab. The dynamics calculations include motion in the azimuthal coordinate although the PES does not depend on ϕ for impact on the top and hollow sites. Large dissociation probabilities (~ 0.9) are found for impact at the hollow site but those for impact at the top site are lower (~ 0.3). Dissociation probabilities for molecules incident with ''helicoptering'' motion ($m_j = j$) are larger than those for molecules with ''cartwheeling'' motion ($m_j = 0$). This differs from the results of previous calculations for impact at the azimuthally corrugated bridge site which predicted comparable probabilities for the two orientations of incident molecules. The dissociation probabilities from fixed-site calculations at the different impact sites are combined to yield an averaged probability which is compared with experiment and the results of six-dimensional quantum calculations. Vibrationally inelastic scattering is predicted to occur primarily for impact at the top site. © *1998 American Institute of Physics.* [S0021-9606(98)00116-0]

I. INTRODUCTION

Experimental investigations have revealed important information about the dissociative chemisorption of H_2 and D_2 on Cu surfaces.[1–19] Experiments measuring the sticking probability as a function of incident translational energy and incidence angle[1–3] established that dissociation is an activated process that obeys normal energy scaling.[4] The translational energy and scattering angle of H_2 desorbing from the surface in the reverse process, associative desorption, were measured in other experiments.[5] Experiments using seeded molecular beams demonstrated that excess energy in the vibrational mode of incident molecules enhances dissociation [vibrationally enhanced dissociation (VED)], lowering the translational energy threshold relative to that for molecules in the ground vibrational state.[6–9] Analysis of the results of associative desorption experiments using the principle of microscopic reversibility has shown that rotational motion hinders dissociation for low values of j, the rotational quantum number, and enhances it for higher j.[10,11] Recent experiments on D_2+Cu(111) measured the alignment of desorbing molecules[12–14] confirming the expected result that molecules with ''helicoptering''-type motion are more reactive than those with ''cartwheeling'' motion. However, the difference in probabilities almost disappears as the collision energy increases.[14] State-selective measurements of D_2 and H_2 scattered from Cu surfaces[9,15–19] showed significant probabilities for vibrationally inelastic scattering (VIS). A mechanism postulated to explain these results invoked a lengthening of the bond as the molecule moved along the reaction path toward a ''late'' barrier, which is quite similar to the mechanism involved in dissociation. Based upon this mechanism and the observation of similarities between the energy dependence of the VIS and dissociation processes, it was proposed[17] that they might occur on similar regions of the potential energy surface.

Theoretical studies using various reduced-dimensional computational models[20–48] have aided in understanding the dynamics of activated dissociation. Two-dimensional (2D) models demonstrated the VED effect for systems with a ''late'' dissociation barrier (i.e., one located in the products channel).[20–25] A portion of the vibrational energy, which initially is in a mode involving motion perpendicular to the reaction path, is converted into energy along the reaction path and is available for use in crossing the dissociation barrier. Three- (3D) and four-dimensional (4D) models including rotational motion demonstrated the importance of including these degrees of freedom to provide a realistic description of the dissociation process.[25–38] Calculations using these models[35] have reproduced the dependence of the dissociation probability on j demonstrating that steric effects are responsible for the decrease in dissociation for low values of j and the ''centrifugal'' effect, in which rotational motion couples with motion along the reaction pathway, for the increase in the dissociation probability for higher j. Predictions from fixed-site calculations using flat surfaces[29,30]

[a)]Electronic mail: rcm@alchemy.nrl.navy.mil

and surfaces with corrugation in the azimuthal coordinate[35,36] are consistent with the observation of enhanced dissociation of helicoptering molecules at low translation energies but the difference is larger than what is observed experimentally for D_2+Cu(111). Calculations modeling impact at a bridge site on the (100) surface using a potential with strong azimuthal corrugation[38] predict comparable dissociation probabilities for cartwheeling and helicoptering molecules, a result that is consistent with experimental observations for D_2+Cu(111) at higher translational energies. Dynamical calculations including parallel translational motion[39–46] have yielded information about the effects of the variation of the height of the dissociation barrier across the surface. Recent calculations on the (100) surface suggest that diffraction data at energies near the height of the barrier can reveal information about the potential energy surface (PES) near the barrier.[46] These calculations showed that dissociation occurs primarily for impacts near bridge and hollow sites while VIS occurs near top sites, a result that is consistent with results of previous fixed-site calculations which suggested that dissociation and VIS should occur at different surface sites.[47,48]

Analysis of the predictions of the various reduced-dimensional models emphasizes the importance of incorporating all the essential degrees of freedom in the computational model in order to realistically describe the dynamics of dissociation. Recently, the results of six-dimensional (6D) quantum mechanical calculations for H_2 dissociation on the Cu(100) (Refs. 49 and 50) and (111) (Ref. 51) surfaces have become available. These results are useful for quantitative comparisons with experiment, the insight they provide on the dissociation dynamics, and as benchmarks for less exact theoretical models.

The PES used in the 6D calculations for the Cu(100) surface[52] was used previously in a series of reduced-dimensional calculations: a 2D calculation for impact at the bridge site with dissociation toward hollow sites,[24] a 4D fixed-site calculation incorporating rotational motion for impact at the bridge site (4D-B),[38] and a 4D calculation with the molecular axis fixed parallel to the surface with parallel translation included ($4D$-XY).[45,46] The calculations described herein extend this series by examining collisions in which the molecular center-of-mass remains fixed above either the hollow or the top sites. The model includes motion of the molecular center-of-mass perpendicular to the surface (Z), the H–H bond distance (r), and rotational motion (θ and ϕ). The potential describing the interaction of the molecule with the surface differs qualitatively from that used in the 4D-B model in that corrugation in the azimuthal coordinate is not included.

The current study was undertaken to shed light upon several important issues in the H_2/Cu(100) system. First, comparison of the energy dependence of the dissociation probabilities predicted by the fixed-site models for impact at bridge, hollow, and top sites will indicate the relative contribution of each site to the overall dissociation probability. Density functional theory (DFT) calculations indicate that, for the high-symmetry sites, the energy barrier is lowest for impact at the bridge site, followed by the hollow and top sites. Since the dynamical threshold, defined as the energy at which the dissociation probability first reaches one-half its saturation value, is closely related to the minimum barrier height,[32,47] the same ordering would be expected for the dynamical thresholds. It would be expected that dissociation would occur at the lowest collision energies only for collisions with impact points near bridge sites. As the energy increases, collisions of molecules at hollow and top sites would begin to contribute to the total dissociation probability. Two-dimensional calculations[46] in which the molecular bond was held fixed parallel to the surface predict that dissociation occurs preferentially at bridge and hollow sites with substantially smaller probabilities for impact at the top site. The present work will determine if this remains the case when rotational motion is included.

A second issue is the importance of VIS for impact at the different sites. The full 6D calculations[49,50] and those using the $4D$-XY[45,46] predict significant probabilities for VIS of ground state H_2. Analysis of the results of 2D calculations showed that VIS occurs exclusively at top sites due to the very late barrier and high curvature of the potential energy surface at this site. The 4D-B calculations[38] predicted probabilities for VIS up to 0.12. In this case, VIS is attributed to collisions in which the molecular axis is tilted slightly away from parallel to the surface. The PES for such orientations exhibits the characteristics associated with VIS: a late barrier and high curvature. The current work investigates collisions at hollow and top sites to determine the extent of VIS when rotational motion is included in the model for these sites.

A third issue concerns the influence of the azimuthal anisotropy of the PES on the dissociation process. As mentioned previously, calculations modeling collisions of H_2 with flat surfaces[29,30] predict much larger dissociation probabilities for collisions in which the incident molecule is rotating with its angular momentum vector perpendicular to the surface (helicoptering motion) than when the angular momentum vector is parallel to the surface (cartwheeling motion). The enhanced dissociation in the former case results from the fact that the molecular orientation is favorable to dissociation (i.e., parallel to the surface). For cartwheeling motion, the molecular axis is parallel to the surface only a fraction of the time so most collisions occur with the molecule in a less than optimal orientation for dissociation. The majority of the collisions result in nonreactive scattering. This dependence on the rotational state of the incident molecule is in qualitative agreement with experimental measurements of the alignment of D_2 desorbing from Cu(111) but the calculations overestimate the magnitude of the effect.[12–14] Furthermore, the calculations predict much larger dissociation probabilities than are observed experimentally. A strong preference for dissociation by helicoptering molecules remains in 4D[35,36] and 6D[51] calculations modeling H_2 on Cu(111) using potentials that include azimuthal corrugation in the PES. Qualitatively different behavior occurs in calculations modeling H_2+Cu(100) with the 4D-B model.[38] In these calculations, the azimuthal dependence of the potential was determined from DFT calculations with the molecular axis pointing toward hollow and top sites. The height of the minimum energy barriers for these orientations is 0.48 and

1.37 eV, respectively. The location of the barriers differs substantially: $r=2.33a_0$ and $Z=1.99a_0$ for the bridge site compared to $r=3.95a_0$ and $Z=2.86a_0$ for the top site. These energetic and geometric differences result in strong corrugation in the azimuthal direction. The dynamics calculations predict comparable dissociation probabilities for the $j=4$, $m_j=4$ and $j=4$, $m_j=0$ initial rotational states. Experimental measurements indicate a slight preference for dissociation by helicoptering D_2 on Cu(111) (Ref. 14) at high collision energies. The dissociation probability computed using the 4D-B model for H_2 in the ground rovibrational state reaches a maximum of only 0.45, comparable to the experimentally obtained saturation value,[4] for collision energies less than 0.95 eV. The source of the qualitative differences between the results of the various computational models may result from differences in the strength of the azimuthal corrugation in the PESs. The current calculations for impacts at hollow and top sites omit corrugation in the azimuthal coordinate and provide additional information about its influence on the orientation dependence of the dissociation probability and the maximum probabilities that are predicted. For the purpose of comparison with our previous work, results are presented for calculations for impact at the bridge site using a PES that omits azimuthal corrugation.

A final issue is the possibility of reproducing the energy dependence of the dissociation probability predicted by 6D calculations by averaging the results of lower dimensional calculations. Good agreement between 6D results for H_2 on Cu(111) and those obtained by averaging results from 4D fixed-site calculations is reported[51] when the latter are adjusted to account for neglect of zero-point vibrational motion in the X and Y directions at the top of the dissociation barrier. Six-dimensional calculations for H_2 with normal incidence on Cu(100) predict that scattered molecules contain significant amounts of energy (~ 0.05 eV) in motion parallel to the surface.[46] This indicates coupling with the translational degrees of freedom and suggests that such an averaging procedure may not reproduce the results of the full 6D calculation for the (100) surface. By combining the results of the hollow and top site calculations reported here with the results of calculations for the bridge site[38] the accuracy of this approximation can be tested for another system.

The computational model, including a brief description of the wave-packet method and the PES, is described in Sec. II. The results of the calculations and a discussion of their significance is given in Sec. III. The conclusions are summarized in Sec. IV.

II. THEORY

The dynamics calculations used a fixed-site model in which the H_2 molecular center-of-mass is fixed above either a hollow (3D-H), top- (3D-T), or bridge site (3D-B) on the Cu(100) surface. The coordinate system is shown in Fig. 1. Within the fixed-site model there is no dependence on the coordinates X and Y so they need not be explicitly included in the Hamiltonian. The dynamics of the Cu atoms is neglected. The Hamiltonian describing the dynamics of the H nuclei is given by

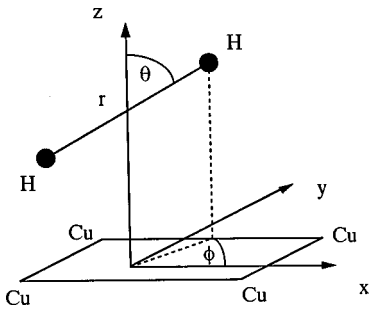

FIG. 1. Coordinate system used in 4D H_2/Cu(100) calculations.

$$\hat{H}=-\frac{\hbar^2}{2M}\frac{\partial^2}{\partial Z^2}-\frac{\hbar^2}{2\mu}\frac{\partial^2}{\partial r^2}+\frac{\hat{j}^2}{2\mu r^2}+V_{3D}(Z,r,\theta), \qquad (1)$$

where M and μ are the total mass and reduced mass of H_2, respectively, and V_{3D} is the interaction potential. It is important to note that although the interaction potential is independent of ϕ this coordinate is included along with θ in $\hat{j}^2$, the square of the rotational angular momentum operator.

The interaction potentials for impact at the three high-symmetry impact sites are multidimensional cuts through a six-dimensional potential[52] used in previous full- and reduced-dimensional dynamics calculations.[24,38,45,46,49,50] In constructing the potentials for each impact site the appropriate values of X and Y were used. A value of $\phi=0$ was used in constructing the potential for impact at each of the three sites. This corresponds to dissociation toward the bridge, bridge, and hollow sites for impact at the hollow, top, and bridge sites, respectively. For impact at a hollow site the potential is written as

$$V_h(Z,r,\theta)=V_{00h}(Z,r)Y_{00}(\theta,0)+V_{20h}(Z,r)Y_{20}(\theta,0), \qquad (2)$$

where Y_{00} and Y_{20} are spherical harmonic functions. The expansion functions are given by

$$V_{20h}=(V_{hb140}-V_{hb90})/[Y_{20}(\theta=140.8°) - Y_{20}(\theta=90°)], \qquad (3)$$

and

$$V_{00h}=[V_{hb90}-V_{20h}Y_{20}(\theta=90°)]/Y_{00}. \qquad (4)$$

In these equations h denotes the site above which dissociation takes place (hollow) and b denotes the site towards which the dissociating atoms move (bridge). V_{hb90} and V_{hb140} are two-dimensional (dependent on Z and r) fits to the results of first-principles density functional calculations for parallel ($\theta=90°$) and tilted ($\theta=140.8°$) orientations. The DFT calculations treated a periodic overlayer of H_2 on a semi-infinite Cu slab. Complete details of the DFT calculations along with the fitting procedure used to obtain the analytic representation of the potential are given in Ref. 52. The 3D potential for dissociation above the top site towards bridge sites, V_t, is obtained using a variant of Eqs. (2)–(4) in which the subscript h is replaced by t and hb is replaced by tb. Similarly, replacing the subscript h with b and hb with bh yields a 3D potential for dissociation above the bridge site toward hollow sites, V_b. Note that the 3D potential used

TABLE I. Barrier heights (eV) and locations in r and Z (a_0).

Site	Dissociation to	Barrier height (eV)	$r(a_0)$	$Z(a_0)$
Bridge	Hollow	0.48	2.33	1.99
Bridge	Top	1.37	3.95	2.86
Hollow	Bridge	0.64	1.86	2.15
Top	Bridge	0.70	2.70	2.62

here for impact at a bridge site differs from the 4D potential that includes azimuthal corrugation used in a previous study.[38] The 4D potential contains an additional term depending on $Y_{22}+Y_{2-2}$ that reflects energetic differences for dissociation toward hollow and top sites. The 3D model calculations for impact on the bridge site were used primarily to determine the importance of the azimuthal corrugation of the Cu surface by comparing results of the 3D and 4D models. The six-dimensional potential energy surface used in the full quantum dynamics calculations uses the 4D potential that includes azimuthal corrugation for impact with the bridge site. The barrier heights and locations are given in Table I.

The details of the computational method used to solve the time-dependent Schrödinger equation are explained in detail elsewhere so they are described only briefly here. The close-coupling wave-packet (CCWP) method[53–55] represents the wave function using an expansion in a set of spherical harmonic functions to describe the rotational degrees of freedom. The dependence on Z and r is represented on a two-dimensional grid. Calculations using rotational basis sets of differing sizes indicate that spherical harmonic functions with relatively large values of j ($j_{\max}=28$) are required to accurately represent the dynamics of the dissociating molecule for large r. The interaction potential matrix is diagonal in m_j, the azimuthal quantum number, so only spherical harmonic functions with m_j equal to m_{j0}, the azimuthal quantum number of the incident H_2 molecule, are included in the expansion. Furthermore, the potential matrix is nonzero only for spherical harmonic functions that differ by $\Delta j=0, \pm 2$. This yields a sparse potential matrix and the computational work associated with the potential term of the Hamiltonian scales as $\sim 3\times j_{\max}/2$.

The size of the two-dimensional grids describing the translational dependence of the wave function is reduced by using L-shaped grids that cover only the regions of coordinate space where the wave function is nonnegligible.[56] The grids extend from $Z=-1.0a_0$ to $Z=27.65a_0$ and from $r=0.4a_0$ to $r=6.6a_0$. The time evolution of the wave function is evaluated using the Chebyshev propagation method.[57] The kinetic energy terms in the Hamiltonian are evaluated using the fast Fourier transform algorithm.[58,59]

The initial wave function represents incident H_2 in a particular state with rotational quantum numbers j_0 and m_{j0}, vibrational quantum number ν_0, and with a distribution of values for the center-of-mass translational momentum centered at $k_{Z0}=10.87a_0^{-1}$. The coordinate space representation of the initial wave packet has a width of $\xi=0.5364a_0$ and is centered at $Z_0=17a_0$. State-to-state transition probabilities were computed by analyzing the scattered wave packet as it passed through the dividing surface defined by $Z=20.75a_0$ using the Balint-Kurti method.[60–63] Quadratic absorbing potentials[64] in the reactants region between $Z=21.05a_0$ and $Z=27.65a_0$ and in the products region between $r=4.8a_0$ and $r=6.6a_0$ were used to prevent reflection of the wave packet from the grid boundaries.

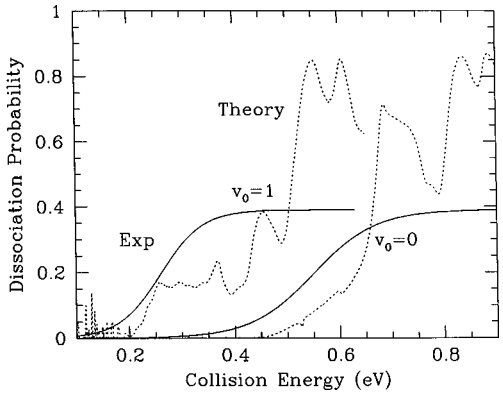

FIG. 2. Dissociation probability of H_2 in the $v_0=0$, $j_0=0$ and $v_0=1$, $j_0=0$ states as a function of collision energy for impact at a hollow site. The probabilities from a fit to experimental measurements (Ref. 4) are shown.

III. RESULTS AND DISCUSSION

The dependence of the dissociation probability on the collision energy for H_2 in the $\nu_0=0$, $j_0=0$ state for impact at hollow and top sites is shown in Figs. 2 and 3, respectively. The dissociation probability at a hollow site is greater than that at a top site throughout the energy range shown indicating that dissociation occurs more readily at the former. This is consistent with the height of the energy barrier at the hollow site being 0.06 eV lower than that at the top site. However, a difference only in the barrier heights would be expected to result primarily in a shift of the dissociation curve along the energy axis but the differences are more extensive than this. For the hollow and top sites the dissociation probability reaches 0.01 (i.e., it becomes somewhat greater than zero) at $E=0.47$ and 0.54 eV, respectively. The difference between these values (0.07 eV) corresponds almost exactly to the difference in the barrier heights at the two sites. Com-

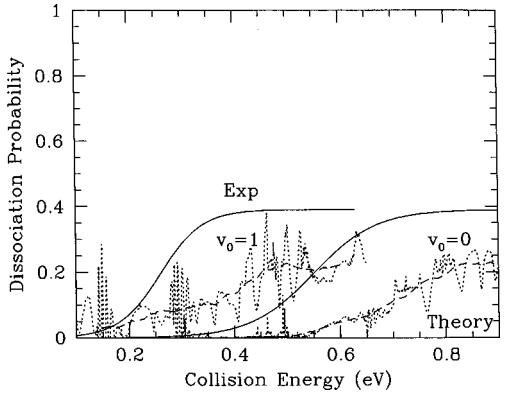

FIG. 3. Dissociation probability of H_2 in the $v_0=0$, $j_0=0$ and $v_0=1$, $j_0=0$ states as a function of collision energy for impact at a top site. The probabilities from a fit to experimental measurements (Ref. 4) and from averaging the computed results over an energy range of 0.1 eV are shown.

parison of Figs. 2 and 3 indicates that the dissociation probabilities at these sites cannot be superimposed simply by a shift in energy. For example, the maximum value of the dissociation probability for impact at a hollow site is 0.87 but is only 0.27 for impact at a top site. As will be discussed more fully later, these dissimilarities reflect differences in the collision dynamics at the two sites that result, for example, in larger probabilities for vibrationally inelastic scattering at the top site than at the hollow site. Both curves exhibit fluctuations that are due, in part, to additional scattering channels opening up[65] and to resonance effects.[46] Although the shapes and locations of these features are of interest, they will not be discussed here.

Experimental measurements of the sticking probability were fit to the functional form

$$P_\nu(E)=\frac{A}{2}\,(1+\tanh\{[E-T(\nu)]/W(\nu)\}), \tag{5}$$

where ν is the initial vibrational state of H_2, A is the saturation value, T is the energetic threshold, and W is the width of the curve.[4] The fitted dissociation probability is shown in Figs. 2 and 3. Although the energy dependence of the computed dissociation probabilities are too complicated to be fit accurately using such a simple function, for the purposes of comparison to the experimental results we define the saturation value as the maximum computed dissociation probability and the dynamical threshold as the lowest collision energy at which the dissociation probability reaches one-half its maximum value. The energetic threshold for the ground vibrational state obtained by fitting to the experimental measurements is 0.58 eV. The computed dynamical thresholds for impact at hollow and top sites are higher, with values of 0.67 and 0.70 eV, respectively. For both sites the energetic threshold is in good agreement with the height of the dissociation barrier at that site. This indicates that the zero-point vibrational energy at the saddlepoint of the potential is approximately equal to that of gas-phase H_2. A similar relation between the dynamical threshold and the barrier height was found in an earlier study[38] examining impact on a bridge site. The experimental saturation value of 0.39 lies between that of the top site (0.27) and that of the hollow site (0.87). Definition of a width for the computed curves is not straightforward due to the structure in the curves.

The computed dissociation probability for H_2 incident in the $\nu_0=1$, $j_0=0$ state for impact at the hollow and top sites is shown in Figs. 2 and 3, respectively, along with the probability obtained from a fit to experimental measurements.[4] For impact at the hollow site (Fig. 2) the computed dissociation probability becomes nonzero for $E\sim 0.2$ eV and, as is the case for the ground state, has a complicated energy dependence. The computed curve is much broader than the experimental curve and the theoretical (0.87) and experimental (0.39) saturation values differ substantially. The computed dynamical threshold is at 0.5 eV and the experimental value is 0.26 eV. Dissociation occurs at lower collision energies for vibrationally excited molecules than for those in the ground vibrational state. A portion of the initial vibrational energy is used to cross the dissociation barrier reducing the amount of center-of-mass translational energy needed. The fraction of the vibrational energy used to cross the barrier, called the vibrational efficacy, is defined as

$$\kappa=\frac{E_0(0)-E_0(1)}{E(\nu=1)-E(\nu=0)}, \tag{6}$$

where $E_0(\nu)$ is the dissociation threshold for initial vibrational state ν and $E(\nu)$ is the energy of gas-phase H_2 in vibrational state ν. The separation between the lowest H_2 gas-phase vibrational levels from the calculated potential is 0.504 eV. Substituting these values into Eq. (6) gives an efficacy of 0.34 for impact at the hollow site which is much lower than the experimental value of 0.64.

The fluctuations in the dissociation probability for collisions at a top site complicate the determination of the saturation value and dynamical threshold. The effects of the fluctuations can be minimized by computing a nominal dissociation probability at each collision energy by averaging over the probabilities within an energy interval surrounding each collision energy. This is a crude computational approximation to an experimental configuration in which the incident beam contains molecules with a distribution of translational energies. Figure 3 shows the result when the dissociation probabilities within 0.05 eV above and below the collision energy are included in the averaging procedure. The resulting curves are significantly smoother and can be compared more readily with the experimental results. The saturation value and energetic threshold for molecules incident in the ground vibrational state are 0.228 and 0.701 eV, respectively. For the first excited vibrational state the respective values are 0.226 and 0.375 eV. Using these values for the dynamical threshold in Eq. (6) yields a value of 0.65 for the vibrational efficacy, in good agreement with the experimental value. The curves obtained by the averaging procedure have a larger width than the experimental curves for both initial states. Application of the averaging method to the results of the calculations for impact at a hollow site gives $\kappa=0.36$ which is essentially the same as the value obtained without averaging.

The trend found in the vibrational efficacies for impact on the hollow (early barrier) site and top (late barrier, see Table I) site is consistent with predictions of calculations examining the influence of potential topology on the vibrational enhancement of dissociation.[23,48] In these calculations, potentials with a late barrier to reaction had a larger vibrational efficacy than potentials with barriers earlier in the products channel.

The dissociation probability for H_2 in the ground rovibrational state from the 3D models is compared with those of other low-dimensional models and a full 6D model in Fig. 4. The 2D results are for impact at a bridge site with the dissociating atoms moving toward hollow sites ($\phi=0°$) and with the internuclear axis fixed parallel to the surface ($\theta=90°$).[24] The molecule follows the most favorable dissociation pathway for the high-symmetry sites. The dissociation probability rises rapidly and saturates at unity for high collision energies. Four-dimensional results are shown for two different models: a model that includes translational motion parallel to the surface but excludes rotation (4D-XY)[45,46] and a fixed-site model for impact on a bridge site that includes rotation

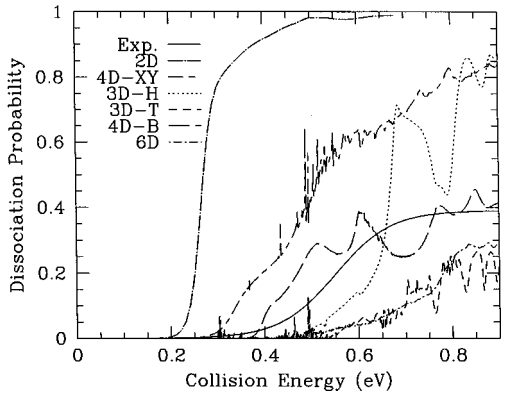

FIG. 4. Dissociation probability of H_2 in the $v_0=0$, $j_0=0$ state as a function of collision energy from the 2D (Ref. 24), 3D-H, 3D-T, 4D-B (Ref. 38), 4D-*XY* (Ref. 46), and 6D (Ref. 49) models.

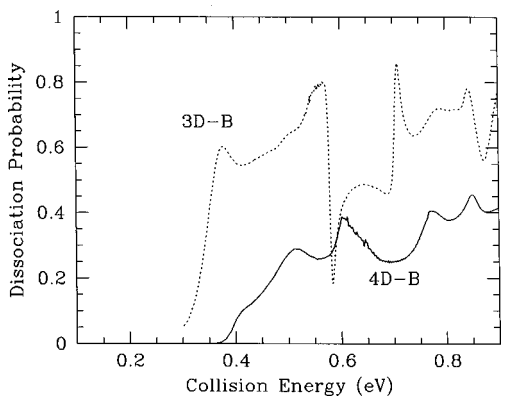

FIG. 5. Dissociation probability of H_2 in the $v_0=0$, $j_0=0$ state as a function of collision energy from the 3D-B and 4D-B (Ref. 38) models.

(4D-B).[38] For both 4D models, the dynamical threshold shifts to higher energies, the saturation value decreases, and the curve broadens. These effects result from an increase in the effective height of the lowest barrier due to quantization of motion in two additional coordinates and to sampling a range of higher barriers. The dynamical thresholds from the 3D-H and 3D-T models are at higher energies than those from the 4D models due to the increased height of the minimum energy barriers for the 3D models relative to those of the 4D models. The saturation value for the 3D-H model is greater than that of the 4D-B model but comparable to that of the 4D-*XY* model. This suggests (as will be demonstrated later in this section) that the lower saturation value in the 4D-B model results from the ϕ dependence of the interaction potential. The 3D-T model predicts a lower saturation value than either of the 4D models. Finally, the dynamical threshold from the 6D calculations is 0.76 eV, higher than that of any of the reduced-dimensional models. This is due to an increase in the effective barrier height because of quantization of energy in five degrees of freedom at the dissociation barrier. The saturation value from the 6D model (0.28) is lower than that of all the models except for 3D-T because reaction is unfavorable for many impact sites and molecular orientations.

To test the hypothesis that the ϕ dependence of the potential in the 4D-B model is responsible for the lower saturation value in that model relative to the 4D-*XY* and 3D-H models, calculations were performed for a 3D model for impact on a bridge site in which the azimuthal corrugation is excluded (3D-B). The variable ϕ is retained within the rotational energy term of the Hamiltonian but the potential is a cut through the 4D-B potential at $\phi=0°$ (a plane perpendicular to the surface passing through the bridge and hollow sites). The energy dependence of the dissociation probability for H_2 in the ground rovibrational state from the 3D-B and 4D-B[38] models is compared in Fig. 5. For a collision energy of 0.3 eV (the lowest impact energy with a significant amplitude in the incident wave packet) the 3D-B model predicts a dissociation probability of 0.05. The dissociation probability increases rapidly to 0.6 for $E=0.37$ eV, decreases slightly for energies up to 0.42 eV, and then gradually increases to 0.8 for $E=0.57$ eV. The computed dynamical threshold is 0.35 eV. Including azimuthal corrugation increases the dynamical threshold to 0.47, decreases the saturation value to 0.4, and broadens the curve. These changes result from an increase in the height of the lowest effective dissociation barrier and an increased sampling of dissociation pathways with higher dissociation barriers. The effective barrier height determines the amount of energy necessary for the molecule to pass over the barrier (although dissociation can occur for lower energies by tunneling). The effective barrier height is calculated by subtracting the asymptotic potential energy of gas-phase H_2 and its zero-point vibrational energy (ZPE) from the sum of the potential energy and ZPE at the saddlepoint of the PES. The PES differences along the minimum energy pathway are the same in both the 3D-B and 4D-B models as is the gas-phase ZPE. However, the ZPE at the saddlepoint is greater for the 4D-B model due to quantization of motion in ϕ. This increases the amount of energy necessary for the molecule to dissociate, shifting the dynamical threshold and collision energy at which dissociation ''turns on'' to higher values than those in the 3D-B model. In the 4D-B model molecules incident with $\phi\neq 0°$ will experience higher energetic barriers (neglecting the fact that ϕ may change as the molecule approaches the surface) than those with $\phi=0°$ (dissociation toward bridge sites). Sampling these higher barriers will shift the dynamical threshold to higher energies and broaden the curve. The saturation

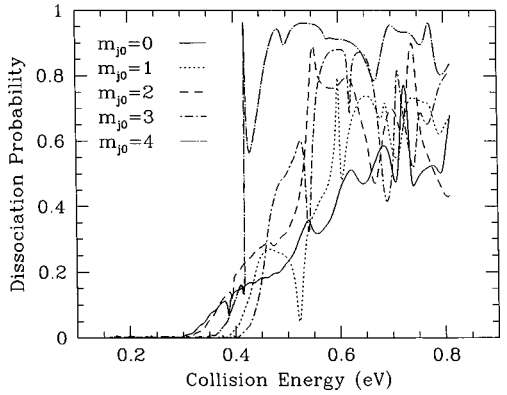

FIG. 6. Dissociation probability of H_2 in the $v_0=0$, $j_0=4$ states as a function of collision energy from the 3D-H model.

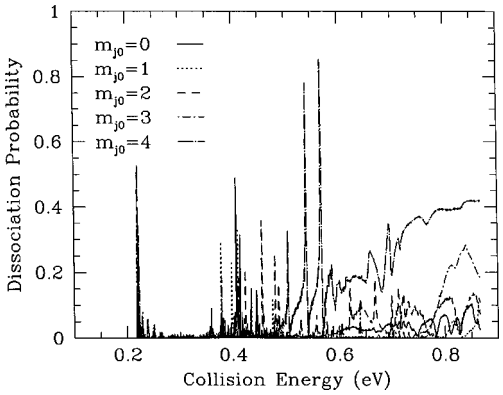

FIG. 7. Dissociation probability of H_2 in the $v_0=0$, $j_0=4$ states as a function of collision energy from the 3D-T model.

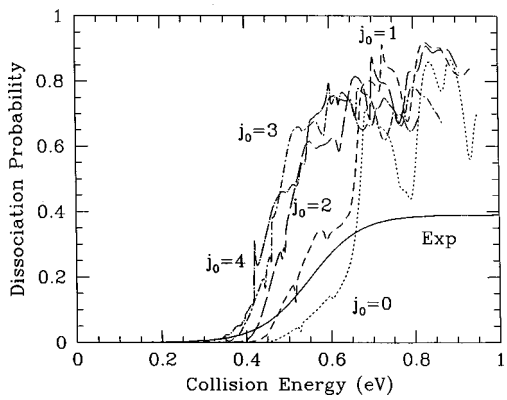

FIG. 9. Orientationally averaged dissociation probabilities for the $j_0 \leqslant 4$ rotational states. A functional fit to the experimentally observed dissociation probability is shown (Ref. 4).

value decreases for the 4D-B model since there is an increased probability for incident molecules with nonoptimal orientations (e.g., $\phi=90°$) to encounter high energy barriers and to scatter back into the gas phase rather than to dissociate.

The dependence of the dissociation probability on collision energy in the 3D-H and the 3D-T models for molecules incident in $j_0=4$ is shown in Figs. 6 and 7, respectively. The results are consistent with those of previous studies using flat[29,30] and corrugated[35,36] surfaces which predict higher reactivities for molecules rotating like helicopters ($m_{j0}=j_0$) than for those rotating like cartwheels ($m_{j0}=0$). This preference is explained by the fact that dissociation occurs only when the molecular bond is nearly parallel to the surface. This condition is met only a small fraction of the time for cartwheeling molecules while helicoptering molecules are in an orientation that is nearly optimal all the time.

The behavior can differ for surfaces with strong azimuthal corrugation. Previous calculations[38] using the 4D-B model predict comparable dissociation probabilities for helicoptering and cartwheeling molecules. These results are are reproduced in Fig. 8 along with results for the 3D-B model (no azimuthal corrugation). The dissociation probability for cartwheeling molecules in the 3D-B model reaches a maximum of about 0.5. Its energy dependence is similar to that of the helicoptering and cartwheeling states from the 4D-B model. The reactivity of helicoptering molecules in the 3D-B model is substantially larger, approaching unity at high collision energies. The similarity between the reactivities for cartwheeling molecules from the two models suggests that the azimuthal corrugation has only a small effect on the dynamics of the dissociation process for cartwheeling molecules. The effect on helicoptering molecules is much larger, with azimuthal corrugation reducing the saturation value, shifting the dynamical threshold to higher energies, and increasing the width of the curve. These same three characteristics are observed as the dimensionality of the computational model increases (cf. Fig. 4) and are attributed to an increase in the height of the minimum barrier and to sampling of higher energy barriers for nonoptimal orientations. Considering impact at a bridge site, the lowest energy pathway occurs when the molecular axis is parallel to the surface ($\theta=90°$) and points toward hollow sites ($\phi=0°$). The wave function representing the final state (two dissociated atoms) will have most of its amplitude centered at adjacent hollow sites and very little amplitude at the top sites because of the high barrier for dissociation for $\phi=90°$. Incident wave functions with the same symmetry would be expected to have the largest dissociation probabilities since their overlap with the final state would be maximal. The wave function representing molecules incident with helicoptering rotational motion will have its largest amplitude for $\theta\sim 90°$ but the distribution in ϕ is isotropic. This nonoptimal symmetry will lead to lower reactivities for azimuthally corrugated surfaces than for those lacking azimuthal corrugation.

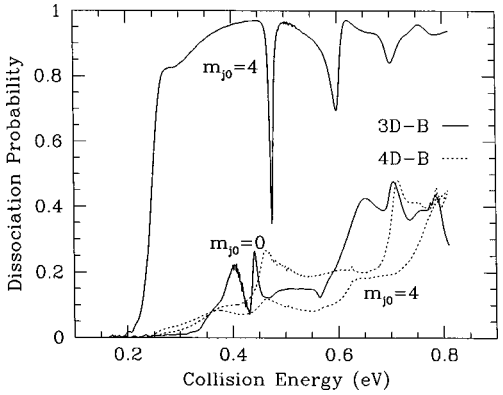

FIG. 8. Dissociation probability of H_2 in the $v_0=0$, $j_0=4$ states as a function of collision energy from the 3D-B and 4D-B (Ref. 38) models.

The energy dependence of the m_j-averaged dissociation probability for $j_0 \leqslant 4$ for impact on a hollow site is shown in Fig. 9. The dynamical threshold and the energy at which dissociation first occurs for each state decrease for increasing j_0. Similar behavior is seen for impact on a top site. In these models rotational energy couples effectively to the reaction coordinate and can be used to aid in crossing the barrier. This is contrary to experimental observations of desorption from the Cu(111) surface that indicate that rotational motion hinders dissociation for low j_0 ($j_0<4$) but assists it for higher values.

The trend found in the 3D-H and 3D-T models is also contrary to that found in calculations on H_2+Cu(100) using

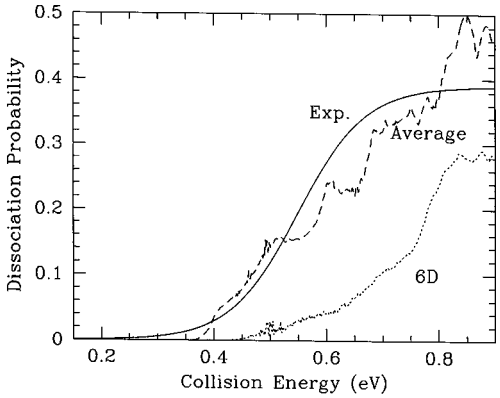

FIG. 10. Dissociation probability from the fit to experiment (Ref. 4), the 6D calculations (Ref. 49), and by weighted averaging of the 3D-H, 3D-T, and 4D-B (Ref. 38) fixed-site results.

the 4D-B model: in these calculations increasing j (to 3 or 4) appears to shift the dynamical threshold up in energy (see Fig. 5 of Ref. 38). Our fixed-site results for H_2+Cu(100) are thus consistent with the experimentally observed dependence of the dynamical threshold on j for the calculation with azimuthal corrugation included, while the opposite trend is found in calculations excluding azimuthal corrugation. This behavior is similar to the results from fixed-site calculations of Darling and Holloway,[35] who found that for a three-dimensional rotor increasing j helps dissociation at low j if the PES does not contain azimuthal corrugation. The experimental trend was, however, recovered when azimuthal corrugation was added to the potential. The interpretation given was that rotational hindering (to which the experimentally observed increase in the dynamical threshold with j at low j is attributed) has a larger effect than an increase in the amount of energy available for reaction with increasing j if the rotational hindering is in two coordinates rather than in just one.

The dissociation probability obtained by a weighted averaging of the results of the fixed-site calculations is shown in Fig. 10. The probabilities from the 4D-B model were multiplied by 0.5 and those from the 3D-H and 3D-T models by 0.25 in computing the average. The saturation value (0.532) and the dynamical threshold (0.670 eV) from the averaged results are higher than those from experiment but the agreement between the curves for energies less than 0.8 eV is quite good. The comparison between the 6D and averaged results is of more interest because of the possibility that averaging fixed-site calculations might provide a computationally less expensive method of modeling dissociation. The saturation value obtained from averaging is almost twice that from the 6D calculations. The dynamical threshold is 0.09 eV lower than that of the 6D calculations.

The averaged results overestimate the dissociation probability relative to the 6D calculations at each energy for several reasons. First, as mentioned previously, the barrier height for each fixed-site calculation omits the zero-point energy for X-Y motion at the barrier. This means that less energy is required for dissociation than in the 6D calculations. Second, it is quite possible that in a typical reaction additional energy is lost to the molecular motion parallel to the surface, because these transitions are excited at the transition state. This possibility is suggested by the finding that the molecules which are reflected have approximately 0.06 eV of energy in parallel translational motion indicating that energy transfer to these modes is facile. A third reason is that the 6D calculations include the effects of dissociation at sites not explicitly treated in the fixed-site models. The barrier heights from the fitted potential at these sites may differ from that based upon a naive expectation that the barrier height should be the average of the barrier heights for which the interpolation is performed. This is true only if the location of the barrier in r and Z is invariant as the impact point changes but this is not the case in fact. As an example, consider a molecule impacting with its center-of-mass midway between a bridge and top site and with the internuclear axis oriented so that it bisects the line segment passing through the bridge and hollow sites. A barrier height of 0.59 eV is obtained by averaging the bridge-to-hollow (0.48 eV) and top-to-bridge (0.70 eV) barriers. The actual barrier height from the fitted potential is 0.75 eV. Similar behavior is seen for other impact points with the ''averaged barrier height'' typically lying lower than that from the fitted potential. These higher barriers in the 6D calculations shift the dynamical threshold upward in energy.

Experimental observations for H_2 and D_2 on the Cu(111) surface indicate comparable probabilities for dissociation and VIS.[17] Calculations using the 4D-XY model with the molecule constrained to remain parallel to the surface ($\theta = 90°$) predict large probabilities for VIS for H_2 incident in the $\nu_0 = 0$ state.[45,46] In calculations using 2D fixed-site models for broadside impact at the bridge, hollow, and top sites VIS occurs only at the top site and the dissociation probabilities are larger at the bridge and hollow sites than at the top site. These results led to the speculation that VIS would occur almost exclusively at top sites even for models that include rotational motion.[46]

Subsequent calculations using the 4D-B model predicted probabilities of up to 0.1 for vibrational excitation for impact at the reactive bridge site, roughly one-fourth the predicted dissociation probability.[38] Analysis using 2D models for this site showed that dissociation occurs for molecules oriented around $\theta = 90°$ and VIS for those tilted slightly away from parallel to the surface ($60° \leqslant \theta \leqslant 80°$). Tilted molecules experience a later barrier and an increased curvature of the reaction path, which offers a possible explanation for the observed greater efficiency for VIS. Nevertheless, it was speculated that collisions with top sites would be more effective in causing VIS than those with bridge sites for a model which also includes the effects of rotational motion.[38] Broadside collisions at the top site are already very effective in causing VIS, and it was considered likely that slightly tilted orientations would also be effective. Collisions with the top site would then be more effective in causing VIS than collisions with the bridge site because broadside collisions contribute to VIS for the top site, but not for the bridge side.

Figure 11 shows the probabilities for VIS for H_2 incident in the ground rovibrational state from the 3D-H and 3D-T sites and reproduces those from the 4D-XY and 4D-B calculations. These calculations confirm that impact at or near top

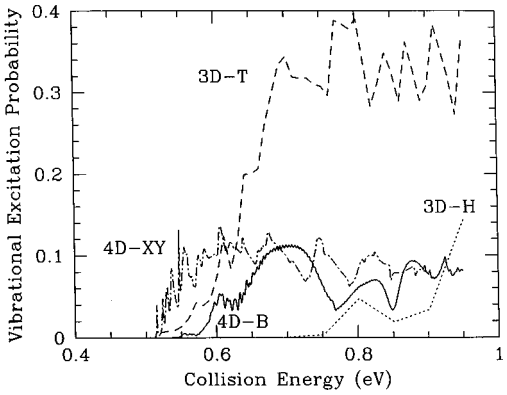

FIG. 11. Probability for vibrationally inelastic scattering ($v_0=0$, $j_0=0 \rightarrow v_0=1$) predicted by the 3D-H, 3D-T, 4D-*XY* (Ref. 46) and 4D-B (Ref. 38) models.

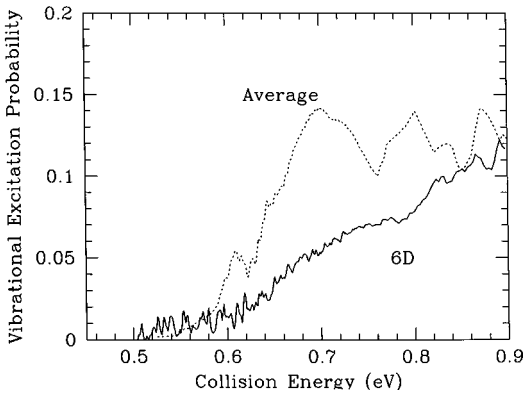

FIG. 12. Probability for vibrationally inelastic scattering ($v_0=0$, $j_0=0 \rightarrow v_0=1$) from the 6D model and by weighted averaging of the 3D-H, 3D-T, and 4D-B (Ref. 38) fixed-site results.

sites produces the largest probabilities for VIS even when rotational motion is included. The maximum VIS probability from the 3D-T model (~ 0.4) is comparable to that from the 2D fixed-site model for broadside collisions.[46] The probabilities for VIS for impact at the bridge and hollow sites are significant when rotational motion is included whereas they are negligible in 2D calculations for molecules oriented with $\theta=90°$. Previously, in Ref. 38, a possible explanation has been offered for the enhancement of vibrational excitation by rotation for the 4D-B results, based on the results of model calculations[47] which showed that VIS can be efficient for potentials in which the reaction path shows a large curvature in front of a late barrier. When the molecule is tilted slightly away from an orientation parallel to the surface, this leads to an increased curvature of the reaction path in front of the barrier, and to the barrier becoming later or even disappearing because the potential becomes increasingly repulsive when the H–H bond lengthens. The combined effect of these changes can be that the molecule is reflected in a vibrationally excited state. The phenomenon observed in the calculations demonstrates the importance of including all essential degrees of freedom in dynamics calculations to accurately describe both nonreactive and reactive collisions. Including the rotational degrees of freedom incorporates a completely new mechanism for vibrational excitation that is neglected in fixed-orientation models with $\theta=90°$.

The energy dependence of the probability for VIS obtained by averaging over the fixed-site models is compared with that from the 6D calculations in Fig. 12. In both cases the probability for VIS becomes nonzero as the collision energy exceeds the separation between the $v=0$ and 1 levels. The averaged results predict probabilities that are as much as twice as large as those from the 6D calculations for midrange energies but are in fairly good agreement at the highest energies shown.

IV. CONCLUSIONS

The dynamics of H_2 impacting at hollow and top sites of a Cu(100) surface was studied using a four-dimensional quantum mechanical model. The potential energy surface used is a fit to the results of density functional theory calculations that used the generalized gradient approximation for a periodic overlayer of H_2 on a Cu slab. The PES is not dependent on the azimuthal angle for impacts at the hollow and top sites. Probabilities for dissociation and vibrationally inelastic scattering were computed as a function of incidence energy for various initial rotational and vibrational states.

Comparison with the results of earlier fixed-site calculations for impact at a bridge site indicates that the amount of collision energy required for dissociation to occur is lowest for the bridge site, followed by the hollow and top sites. This agrees with the ordering of the height of the energy barriers for the different sites. Throughout most of the energy range examined, the dissociation probability for a collision at a hollow site exceeds that for impact at a top site, for which vibrational excitation competes efficiently with reaction. Excess vibrational energy in the incident molecule reduces the amount of collision energy required for dissociation. The effectiveness of the vibrational energy is quantified by the vibrational efficacy which is 0.34 and 0.65 for the hollow and top sites, respectively. The trend in these values is consistent with the hollow site exhibiting an earlier barrier to reaction than the top site.

Significantly larger dissociation probabilities are observed for molecules impacting the surface with helicopter-type rotational motion than for those rotating like cartwheels. Molecules with helicopter-type rotation approach the surface with the molecular axis aligned nearly parallel to the surface, which is the preferred orientation for dissociation on a surface lacking azimuthal corrugation. This result is different than that from calculations examining impact at the azimuthally corrugated bridge site which predict comparable dissociation probabilities for the two types of rotational motion. Dynamics calculations with the azimuthal corrugation of the PES at the bridge site eliminated show the same qualitative differences between helicoptering and cartwheeling rotational motion as are obtained at the hollow and top sites. Taken together, these results indicate that azimuthal corrugation has a strong influence on the dependence of the dissociation probability on the m_j quantum number. Its overall effect is to reduce the dissociation probability for molecules incident with helicoptering rotational motion.

The probabilities for vibrationally inelastic scattering at

the high-symmetry impact sites examined are inversely related to the dissociation probabilities at the sites. The largest probability for VIS occurs at the top site. This result is consistent with the results of the 4D-XY model[46] which included the effects of parallel translational motion but neglected rotational motion. These new results indicate that rotational motion has only a limited influence on the dynamics of VIS at top sites. On the other hand, inclusion of rotational motion was found to significantly increase VIS in collisions with the bridge and hollow sites, revealing a mechanism for vibrational excitation in which the molecule is slightly tilted away from the orientation parallel to the surface.

ACKNOWLEDGMENTS

The work at NRL was supported by the Office of Naval Research through the Naval Research Laboratory. This work was supported in part by a grant of HPC time from the U.S. Army Corp of Engineers Waterway Experiment Station Cray C-90 and the Naval Oceanographic Office/MSRC Program Cray T-90. The work of one of the authors (G.J.K.) was supported by the Royal Netherlands Academy of Arts and Sciences and by a grant of computer time by the Dutch National Computing Facilities Foundation (NCF). This work was also supported by The Netherlands Foundation for Chemical Research (SON) with financial aid from The Netherlands Organization for Scientific Research (NWO).

[1] M. Balooch, M. J. Cardillo, D. R. Miller, and R. E. Stickney, Surf. Sci. **46**, 358 (1974).
[2] G. Anger, A. Winkler, and K. D. Rendulic, Surf. Sci. **220**, 1 (1989).
[3] C. T. Rettner, D. J. Auerbach, and H. A. Michelsen, Phys. Rev. Lett. **68**, 1164 (1992).
[4] H. A. Michelsen and D. J. Auerbach, J. Chem. Phys. **94**, 7502 (1991).
[5] G. Comsa and R. David, Surf. Sci. **117**, 77 (1982).
[6] B. E. Hayden and C. L. A. Lamont, Phys. Rev. Lett. **63**, 1823 (1989).
[7] H. F. Berger, M. Leisch, A. Winkler, and K. D. Rendulic, Chem. Phys. Lett. **175**, 425 (1990).
[8] B. E. Hayden and C. L. A. Lamont, Surf. Sci. **243**, 31 (1991).
[9] D. J. Auerbach, C. T. Rettner, and H. A. Michelsen, Surf. Sci. **283**, 1 (1993).
[10] H. A. Michelsen, C. T. Rettner, D. J. Auerbach, and R. N. Zare, J. Chem. Phys. **98**, 8294 (1993).
[11] C. T. Rettner, H. A. Michelsen, and D. J. Auerbach, J. Chem. Phys. **102**, 4625 (1995).
[12] D. Wetzig, M. Rutkowski, R. David, and H. Zacharias, Europhys. Lett. **36**, 31 (1996).
[13] S. J. Gulding, A. M. Wodtke, H. Hou, C. T. Rettner, H. A. Michelsen, and D. J. Auerbach, J. Chem. Phys. **105**, 9702 (1996).
[14] H. Hou, S. J. Gulding, C. T. Rettner, A. M. Wodtke, and D. J. Auerbach, Science **277**, 80 (1997).
[15] A. Hodgson, J. Moryl, and H. Zhao, Chem. Phys. Lett. **182**, 152 (1991).
[16] A. Hodgson, J. Moryl, P. Traversaro, and H. Zhao, Nature (London) **356**, 501 (1992).
[17] C. T. Rettner, D. J. Auerbach, and H. A. Michelsen, Phys. Rev. Lett. **68**, 2547 (1992).
[18] C. T. Rettner, H. A. Michelsen, and D. J. Auerbach, Faraday Discuss. Chem. Soc. **96**, 17 (1993).
[19] M. Gostein, H. Parhikhteh, and G. O. Sitz, Phys. Rev. Lett. **75**, 342 (1995).
[20] M. Hand and S. Holloway, Surf. Sci. **211/212**, 940 (1989).
[21] J. Harris, Surf. Sci. **221**, 335 (1989).
[22] M. R. Hand and S. Holloway, J. Chem. Phys. **91**, 7209 (1989).
[23] D. Halstead and S. Holloway, J. Chem. Phys. **93**, 2859 (1990).
[24] G. Wiesenekker, G. J. Kroes, E. J. Baerends, and R. C. Mowrey, J. Chem. Phys. **102**, 3873 (1995); *ibid.* **103**, 5168 (1995).
[25] S. Holloway, J. Phys.: Condens. Matter **3**, S43 (1991).
[26] U. Nielsen, D. Halstead, S. Holloway, and J. K. Norskov, J. Chem. Phys. **93**, 2879 (1990).
[27] A. J. Cruz and B. Jackson, J. Chem. Phys. **94**, 5715 (1991).
[28] J. Sheng and J. Z. H. Zhang, J. Chem. Phys. **96**, 3866 (1992).
[29] J. Sheng and J. Z. H. Zhang, J. Chem. Phys. **97**, 6784 (1992).
[30] J. Sheng and J. Z. H. Zhang, J. Chem. Phys. **99**, 1373 (1993).
[31] P. Saalfrank and W. H. Miller, J. Chem. Phys. **98**, 9040 (1993).
[32] R. C. Mowrey, J. Chem. Phys. **99**, 7049 (1993).
[33] J. Dai, J. Sheng, and J. Z. H. Zhang, J. Chem. Phys. **101**, 1555 (1994).
[34] J. Dai and J. Z. H. Zhang, Surf. Sci. **319**, 193 (1994).
[35] G. R. Darling and S. Holloway, J. Chem. Phys. **101**, 3268 (1994).
[36] J. Dai and J. Z. H. Zhang, J. Chem. Phys. **102**, 6280 (1995).
[37] W. A. Diño, H. Kasai, and A. Okiji, Phys. Rev. Lett. **78**, 286 (1997).
[38] R. C. Mowrey, G. J. Kroes, G. Wiesenekker, and E. J. Baerends, J. Chem. Phys. **106**, 4248 (1997).
[39] D. Halstead and S. Holloway, J. Chem. Phys. **88**, 7197 (1988).
[40] G. R. Darling and S. Holloway, Chem. Phys. Lett. **191**, 396 (1992).
[41] G. R. Darling and S. Holloway, J. Chem. Phys. **97**, 5182 (1992).
[42] G. R. Darling and S. Holloway, Surf. Sci. **304**, L461 (1994).
[43] A. Gross, J. Chem. Phys. **102**, 5045 (1995).
[44] A. Gross, B. Hammer, M. Scheffler, and W. Brenig, Phys. Rev. Lett. **73**, 3121 (1994).
[45] G. J. Kroes, G. Wiesenekker, E. J. Baerends, and R. C. Mowrey, Phys. Rev. B **53**, 10 397 (1996).
[46] G. J. Kroes, G. Wiesenekker, E. J. Baerends, R. C. Mowrey, and D. Neuhauser, J. Chem. Phys. **105**, 5979 (1996).
[47] G. R. Darling and S. Holloway, J. Chem. Phys. **97**, 734 (1992).
[48] G. R. Darling and S. Holloway, Surf. Sci. **307–309**, 153 (1994).
[49] G. J. Kroes, E. J. Baerends, and R. C. Mowrey, Phys. Rev. Lett. **78**, 3583 (1997).
[50] G. J. Kroes, E. J. Baerends, and R. C. Mowrey, J. Chem. Phys. **107**, 3309 (1997).
[51] J. Dai and J. C. Light, J. Chem. Phys. **107**, 1676 (1997).
[52] G. Wiesenekker, G. J. Kroes, and E. J. Baerends, J. Chem. Phys. **104**, 7344 (1996).
[53] R. C. Mowrey and D. J. Kouri, Chem. Phys. Lett. **119**, 285 (1985).
[54] R. C. Mowrey and D. J. Kouri, J. Chem. Phys. **84**, 6466 (1986).
[55] D. J. Kouri and R. C. Mowrey, J. Chem. Phys. **86**, 2087 (1987).
[56] R. C. Mowrey, J. Chem. Phys. **94**, 7098 (1991).
[57] H. Tal-Ezer and R. Kosloff, J. Chem. Phys. **81**, 3967 (1984).
[58] M. D. Feit, J. A. Fleck, Jr., and A. Steiger, J. Comput. Phys. **47**, 412 (1982).
[59] D. Kosloff and R. Kosloff, J. Comput. Phys. **52**, 35 (1983).
[60] G. G. Balint-Kurti, R. N. Dixon, and C. C. Marston, J. Chem. Soc., Faraday Trans. **86**, 1741 (1990).
[61] C. C. Marston, G. G. Balint-Kurti, and R. N. Dixon, Theor. Chim. Acta **79**, 313 (1991).
[62] G. G. Balint-Kurti, R. N. Dixon, and C. C. Marston, Int. Rev. Phys. Chem. **11**, 317 (1992).
[63] R. C. Mowrey and G. J. Kroes, J. Chem. Phys. **103**, 1216 (1995).
[64] T. Seideman and W. H. Miller, J. Chem. Phys. **96**, 4412 (1992).
[65] A. D. Kinnersly, G. R. Darling, S. Holloway, and B. Hammer, Surf. Sci. **364**, 219 (1996).